

## Article

# A GIS-Based Index of Physical Susceptibility to Flooding as a Tool for Flood Risk Management

Francis Miranda <sup>1,\*</sup>, Anna Beatriz Franco <sup>2</sup>, Osvaldo Rezende <sup>1</sup>, Bruno B. F. da Costa <sup>3,\*</sup>, Mohammad Najjar <sup>1</sup>, Assed N. Haddad <sup>1</sup> and Marcelo Miguez <sup>1,2,4</sup>

<sup>1</sup> Programa de Engenharia Ambiental, Universidade Federal do Rio de Janeiro, Rio de Janeiro 21941-909, Brazil; omrezende@poli.ufrj.br (O.R.); mnajjar@poli.ufrj.br (M.N.); assed@poli.ufrj.br (A.N.H.); marcelomiguez@poli.ufrj.br (M.M.)

<sup>2</sup> Programa de Engenharia Civil, Universidade Federal do Rio de Janeiro, Rio de Janeiro 21941-450, Brazil; annabfranco@poli.ufrj.br

<sup>3</sup> Instituto Politécnico, Universidade Federal do Rio de Janeiro, Macaé 27930-560, Brazil

<sup>4</sup> Programa de Engenharia Urbana, Universidade Federal do Rio de Janeiro, Rio de Janeiro 21941-909, Brazil

\* Correspondence: francismiranda@poli.ufrj.br (F.M.); bruno.barzellay@macae.ufrj.br (B.B.F.d.C.)

**Abstract:** The identification and classification of flood-prone areas comprise a fundamental step in the Flood Risk Management approach, providing subsidies for land use planning, floodproofing policies, the design of mitigation measures and early warning systems. To address this issue, a frequently used preliminary tool is the flood susceptibility mapping of a region using a range of widely available data. Therefore, the present study introduces an index-based approach able to qualitatively assess flood-prone areas, named Physical Susceptibility to Floods Index (PhySFI), based on a multi-criteria decision-making method and developed in a GIS environment. The methodology presupposes a critical discussion of variables commonly used in other flood indexes, intending to simplify the proposed representation, and emphasizes the role of the user/modeler. PhySFI is composed of just four indicators, based on physical parameters of the assessed environment. This index was developed and first applied in the city of Rio de Janeiro, as part of the Rio de Janeiro Climate Change Adaptation Plan. The validation process was based on a comparative analysis with flood extent and height simulated by the hydrodynamic modeling of four watersheds within the study area, with different urbanization processes for each one. The results indicate that the index is a powerful preliminary tool to assess flood-prone areas in coastal cities.

**Keywords:** flood risk management; MCDM; GIS; flood susceptibility mapping



**Citation:** Miranda, F.; Franco, A.B.; Rezende, O.; da Costa, B.B.F.; Najjar, M.; Haddad, A.N.; Miguez, M. A GIS-Based Index of Physical Susceptibility to Flooding as a Tool for Flood Risk Management. *Land* **2023**, *12*, 1408. <https://doi.org/10.3390/land12071408>

Academic Editor: Adrianos Retalis

Received: 23 June 2023

Revised: 6 July 2023

Accepted: 12 July 2023

Published: 13 July 2023



**Copyright:** © 2023 by the authors. Licensee MDPI, Basel, Switzerland. This article is an open access article distributed under the terms and conditions of the Creative Commons Attribution (CC BY) license (<https://creativecommons.org/licenses/by/4.0/>).

## 1. Introduction

Floods can be characterized as the natural disaster with the highest frequency, the largest number of people affected and the third biggest cause of economic losses, behind storms and earthquakes [1–3]. Between 2000 and 2021, floods represented 40% of all natural disasters, reaching 50% of the annual amount in 2006 and 2021. Asian countries are the most affected, followed by South America [3,4]. At the end of 2021, approximately 56% of the world's population lived in urbanized areas. In Brazil, this percentage is around 87% [5]. The main local impacts associated with the urbanization process in the urban water cycle are the reduction in vegetal interception, evapotranspiration, and infiltration, and runoff increases in volume and velocity, mainly as a result of vegetation removal, soil paving, interventions in the natural drainage and the construction of artificial drainage systems [6].

Although flood events are a natural phenomenon usually responsible for a series of ecosystem services [7], their interactions with urban aspects, such as population increase in susceptible areas and urban sprawl, tend to explain the escalation of associated negative impacts.

In developing countries, cities may continue to occupy floodplains without proper urban planning and reproducing a hygienist approach in stormwater systems [8]. Failures in drainage systems functioning in urban areas directly affect daily routines and may promote disruption and losses in a series of urban systems such as housing, energy, water supply, sewage, mobility, community facilities and economy, among others, creating a cascade of effects [8,9].

It is difficult to produce sustainable urban tissue when flooding is capable of affecting almost all urban systems, directly or indirectly, being able to degrade the urban environment and impoverish the local population.

Considering the context of the Flood Risk Management (FRM) approach, an anticipated risk analysis is a strategic demand for more resilient cities in current and future adverse scenarios of increasing urbanization and climate change [10]. The identification and classification of flood-prone areas comprise a fundamental step in the FRM approach, providing subsidies for land use planning, floodproofing policies, mitigation measures and early warning systems, among others [11].

However, robust flood risk analysis can be a highly demanding task, mainly in developing countries where available data related to socioeconomic, environmental and field aspects face problems like low-quality information, low spatial coverage and short time series. The lack of specialized technical teams also aggravates this framework. In addition, even when considering an ideal situation of data availability (more likely to occur in developed countries), before detailing the risk analysis it may be useful to have a preliminary tool to hierarchize priority areas to be studied first.

In this sense, preliminary mapping tools can provide subsidies for urban planning and for detailed urban water management using the few variables available. Flood Hazard Mapping (FHM) aims to represent at least one flooding characteristic among flood depth, spatial flooding extent, flooding duration, damages and losses associated with a return period in the region of interest. It can be generated from knowledge on recent historical floods, from geological and geomorphic evidence, aerial photography, satellite imagery and running hydrologic–hydrodynamic models [11,12] and by using quantitative and semi-quantitative Multi-Criteria Decision Making (MCDM) methods [13,14].

A calibrated and validated hydrologic–hydrodynamic model tends to be the most efficient decision support tool available since it allows the simulation of distributed interventions and the comparison of results in different scenarios. Nevertheless, their development requires expensive field data and significant efforts, as previously mentioned. Rio de Janeiro, for example, is a coastal city with more than 40 urbanized watersheds.

To address this issue, a frequently used preliminary tool in FRM is Flood Susceptibility Mapping (FSM). FSM can be defined as the probability of flood occurrence based on geographical features of the considered region [13].

In addition to providing an overall footprint of the study area, highlighting the main problematic catchments, a physical susceptibility analysis can also identify potential areas for wetlands, reservoirs and multifunctional landscapes, as well as showing areas that are susceptible to flooding but not frequently flooded (due to already implemented mitigation measures), indicating possible residual risk areas.

Considering FSM as a relatively incomplete but useful analysis based on a preliminary flood risk management approach, this study aims to present a simplified method using only four indicators to build the Physical Susceptibility to Floods Index (PhySFI). The main contribution of the present study consists of the reduced number of representative Flood Conditioning Factors (FCFs) in comparison with other, similar studies. The development of a new, reduced set of FCF emphasizes the role of the modeler in the interpretation of physical phenomena both in the hydrologic–hydrodynamic modeling step and in the choice of indicators, normalization classes, weights and the final equation in the MCDM method adopted. The proposed index was developed and first applied in the city of Rio de Janeiro, as part of the Rio de Janeiro Climate Change Adaptation Plan 2040 [14]. The city comprises 1.200 km<sup>2</sup>, aggregating more than 40 catchments and approximately 6.7 million inhabitants.

The PhySFI validation process was based on a comparison with hydrologic–hydrodynamic model results of the depth and extent of four basins within the study area. For planning purposes, a future scenario considering climate change impacts was developed to support the prediction of aggravation conditions on the susceptibility mapping procedure.

## 2. Literature Review

### 2.1. Flood Risk Management

Considering the definition given by UNESCO, Flood Risk can be defined as a combination of the flood hazard and its associated consequences reaching a socioeconomic system [10]. Hazard can be defined as the physical component of risk, given by a defined rainfall and its transformation process into runoff through the floodway along the watershed. Physical characteristics of the watershed, such as slope, land use, drainage density and urbanization, among others, imply flood characteristics such as water depth, flooding extent, flow velocity and flood duration, for example [15,16]. The consequences are related to the exposure and vulnerability aspects of socioeconomic systems [17]. Vulnerability can be divided into economic value, susceptibility to damage and resilience [18,19].

In this sense, studies that do not include flood characteristics should not be named as Flood Hazard Mapping (FHS). Within the same reasoning, a Flood Susceptibility Mapping (FSM), as a preliminary step, should not include flood characteristics.

Unlike other natural disasters, such as hurricanes and earthquakes, many types of floods allow a set of measures to be adopted in the physical environment (watershed) in order to modify the runoff generation process, allowing flood patterns to be changed in time and space. In this sense, it is possible to act to reduce the consequent hazard (inundation) for the same triggering event (precipitation). Rainfall characteristics are common FCFs used in flood indexes. However, considering rainfall in a static analysis introduces a complex issue if a flooded area does not necessarily have a direct relation to where the precipitation itself falls. Water flows through a path in the direction of valley zones or sinks, promoting floods where the topography favors them and not exactly in the precipitation area.

In this context, this paper focuses on the susceptibility related to the physical environment and not the susceptibility related to socioeconomic aspects, which makes up the vulnerability calculation. The words “trend” or “propensity to flooding” can be considered good synonyms to convey this idea.

### 2.2. Types of Floods

Floods can be defined as “the temporary covering by water of land not normally covered by water”, and their driving forces can vary significantly [20]. For example, coastal floods are usually caused by storm surges, wave overtopping or tsunamis. Fluvial floods are induced by rainfall and exceed the main channels’ capacity, in which their ranges can vary gradually from lowland floods to flash floods; pluvial floods are caused by rainfall in urban areas, and groundwater floods by exfiltration. Floods can also be caused by snow-melt and dam failure, among other things [10,16,21–23]. Despite having the same element as a triggering factor, the scope of mitigation measures and land restrictions imposed on an area susceptible to slow-rise flooding will be considerably different from those subjected to frequent flash floods.

By defining aspects associated with different types of floods, actors that participate in the decision-making process can readily distinguish specific tools and available management options to deal with flood risks [17]. According to [21], a more comprehensive evaluation should consider more than one factor, including the spatial patterns of the causative factors of flooding as well as atmospheric and catchment conditions. In this context, this paper is focused on representing fluvial floods on floodplains of coastal cities where sea level variations associated with storm surges, astronomical tides or elevation represent an aggravating impact factor.

### 2.3. GIS and MCDM in Flood Risk Management

Studies utilizing the combination of GIS and MCDM for flood applications have been published since the 1990s [11,24,25]. MCDM applications require criteria to be grouped, standardized and weighted, enhancing work interaction between scientific fields [7].

In a recent review involving flood indexes [13], the authors supported the view that MCDM methods have shown the “capability of integrating stakeholder’s input with less complex processing, less input data requirement, accurate results, and decreased uncertainty”.

Physical features such as slope, geology, distance to the main river network, land use and land cover (LULC), terrain elevation, geology and runoff generation are commonly used as indicators in flood susceptibility indexes [26–31]. Other studies have explored earth observation and remote sensing to detect frequently flooded areas [12,31]. Flood indexes can also be developed to characterize flood types (flash floods or riverine floods) using hydrograph results from hydrodynamic catchment modeling [32]. The combination of hazards and consequences of a given flood, creating a Flood Risk Index, is also a common application [33,34], and more recently flood resilience analyses and indexes have been gaining space in the literature [18,19,35–38].

Kazakis et al. [27] presented a weight review of a Flood Hazard Index (FHI) which incorporated a sensitivity analysis and renamed the index FHI-S. Using the same seven FCFs as in FHI—flow accumulation, geology, land use, elevation, slope, distance from network drainage (DFND) and rainfall (FIGUSED-S method)—in an Analytic Hierarchy Process (AHP), the results obtained showed differences in the choice of the weights. On a 0–10 scale, elevation became the most important factor, instead of flow accumulation, changing its weight from 2.1 to 3.0. Distance for drainage network sustained second place, but changed weight from 2.1 to 2.5, followed by slope, in third place, changing its weight from 0.5 to 1.6, the highest percentage change, occupying the place previously given to elevation. Flow accumulation changed from 3.0 to 1.2 and the other indicators received weights lower than 1. For example, the geology parameter received a weight of 2% in FIGUSED and 4% in FIGUSED-S.

Tehrany et al. (2013; 2014; 2015) developed different methodologies to assess flood hazard using a decision tree (DT) [28], a bivariate and multivariate statistical model [29] and machine learning Kernel type [30]. In the first method, ten FCFs were used: elevation, slope, curvature, stream power index (SPI), topographic wetness index (TWI), distance from network drainage (DFDN), geology, rainfall, land use/cover and soil and surface runoff. The last incorporated a support vector machine (SVM) technique in four Kernel types and the Frequency Ratio (FR) method with eleven FCFs. As a result, the parameters of elevation and slope factors were considered the most influential factors in all Kernel types.

In all mentioned studies [27–30], flood inventory was also given by points indicating historical events. They also highlighted the flood susceptibility assessment as a preliminary step in flood risk management, considering the importance of hydrodynamic modeling as a next step.

Using ten FCFs, Mahmoud and Gan [39] presented a flood susceptibility index with flow accumulation, runoff and soil type as the most influential factors. These results differed from other studies mentioned and, after a sensitivity analysis, the authors concluded that flood susceptibility maps should include more than six FCFs, while other studies suggest that a reduced number of independent FCFs can achieve accurate results [40].

The fact that historically observed flood points are located in high slope zones calls for attention. Pham et al. (2020) discussed different methods and performed a classification between a flash flood and a non-flash flood event before developing a GIS-based approach for flash flood susceptibility assessment [41].

An example of an index with only four FCFs was developed for a stretch of river in Iran [39]. The authors applied an Analytical Hierarchy Process (AHP) and compared the results with flood extent and depths obtained by hydrological–hydrodynamic modeling using HEC-RAS for 50-year and 100-year rainfall events. The FCFs chosen were slope, distance from drainage network (DFDN), LULC and altitude/elevation, and they received weights of 0.138, 0.232, 0.546 and 0.084, respectively. The final index was composed of a sum of normalized weights and normalized ratings for each cell of a 30 m horizontal resolution raster layer.

#### 2.4. Climate Change Impacts

Considering the many areas in which water plays a key role, the impact of climate change combined with urban growth implies even more complex challenges in the Integrated Urban Water Management approach (IUWM) [42–44]. Population growth alone is likely to put more people at risk of flooding, regardless of alterations brought about by changes in climate conditions. However, the impacts of future floods will depend on the adaptive choices adopted concerning event projections [2].

Climate change impacts tend to increase the frequency and severity of intense rainfalls, produce higher mean sea levels, increase storm surges and aggravate hazards in general terms. On the other hand, changes in land use and urbanization increase the vulnerability of socioeconomic systems. As a result, climate change represents a concrete threat to higher flood risks, mainly in developing countries [45] where infrastructure provision can be insufficient and adaptation discussions can be put to the end of the line in favor of basic needs, like sanitation and habitation gaps.

Some traditional structural measures adopted without considering future risk analysis can be inefficient. Intensity–Duration–Frequency (IDF) must be frequently updated and new design projects should be more flexible, using recent data associated with conservative safety factors [46].

In order to promote adaptations to climate change, it is important to assess the possible consequences of future conditions. Since it is a difficult task, mainly due to the inherent doubts about what will in fact happen, this is possible through the use of a series of prediction techniques and tools, such as the construction of scenarios and the use of climate models. In this sense, adaptation measures classified as “no regrets” tend to be used as planning strategies to be adopted in the short term.

### 3. Materials and Methods

The role of modelers in understanding the physical phenomenon and their knowledge about the study area assumes crucial importance in modeling complex systems. Cunge [47] discussed the importance of physical interpretation, and the understanding of the assumed hypothesis of the fundamental equations in flood modeling has been losing importance over decades of models and computational techniques’ development.

Sousa et al. [48] compared two different flood modeling strategies with different levels of effort and computational costs in an urban basin. The authors concluded that efforts directed at physical interpretation and representation in the mathematical modeling process could lead to more simple and efficient model approaches, not necessarily requiring the most advanced technologies or the most sophisticated models.

The Physical Susceptibility to Floods Index (PhySFI) is based on an MCDM approach and developed in a GIS environment. The method presupposes a critical discussion of what could be the minimum significant and representative set of variables commonly used and works by choosing indicators, normalization classes, weights and the final equation itself. PhySFI is composed of just four indicators based on the physical characteristics of the environment (natural and built), involving elevation, slope, distance from the major drainage network and land use. The choice of these indicators was influenced by [42] and involves practical observations: the terrain slopes are one of the most important characteristics for mapping flooding (only nearby plain areas are effectively floodable); the distance to the

major drainage network reflects the threat represented by overflows; the terrain elevation accounts for flow accumulation and additional restrictions imposed by tides and backwater effects (particularly important to coastal cities); and land use impacts runoff generation, which can imply increased flooding (represented by the runoff coefficient).

The land use indicator is usually associated with future urban planning scenarios, but it can also be used indirectly to represent possible climate changes affecting the rainfall intensity. Once the rainfall intensity increase rate is estimated, this increasing rate can be simulated by modifying the runoff coefficient accordingly, since the final effect over the generated discharge will be the same when compared to a direct increase in the rainfall intensity. That is, mathematically, as runoff is given by the product of the rainfall intensity by land use conditions and drainage area, if the multiplier of rainfall increase is applied to the runoff coefficient, it can simulate a rise in the runoff generation and represent a climate change effect. In the same way, the elevation indicator can be adapted to better represent estuaries, coastal areas and sea level variations in climate change scenarios. In the present paper, the current situation and future scenarios with climate change effects were developed.

Conceptually speaking, the main idea behind the proposed metrics is that densely occupied coastal plains near water courses subjected to tidal effects should be represented as the worst areas in terms of susceptibility to floods. The normalization classes and weights will be adjusted by comparison with fluvial flood extent and depths simulated by a hydrologic–hydrodynamic model of four watersheds within the study area. Many studies use historical flooding spots to calibrate or validate flood models or indexes [28–30,39,41,49]. Once flood events have intrinsic parameters such as height, spatial extent, etc., characterizing a flood through a discrete point tends to be a rough approximation, although valid in the context of data scarcity.

The software used to simulate floods was MODCEL [50,51], a quasi-2D model in which the modeling domain is divided into irregular cells forming a flow network connected by 1D equations such as full Saint-Venant dynamic equation, crested weirs, culverts and orifices, among others. The different types of cells represent the natural and artificial watercourses, streets, parks, urbanized and rural floodplains and galleries, among others, in such a way that surface and subsurface layers can be linked.

Once the cell division process of the modeling domain is executed by the modeler, the level of experience in the physical interpretation of the built environment assumes crucial importance and introduces a complex issue. The user must interpret terrain geometric characteristics and define hydraulic parameters for each cell, as well, before creating a flow network between different terrain layers.

An extensive discussion about the role of the modeler in flood modeling is presented in [48]. The choice for this model is due to the practicality of using a known open model that was developed by this research group. However, any other similar model can be used when replicating this method.

A comparison and discussion between modeled flood extent and depths with PhySFI final formulation results can be conducted by using the official Brazilian statistic grid as the reference spatial unit. A similar comparison between hydrodynamic modelling and MCDM flood indexes can be found in [52,53].

The PhySFI values range from 0 to 100 and the classes were divided into 0–20 (very low susceptibility), 20–40 (low susceptibility), 40–60 (medium susceptibility), 60–80 (high susceptibility) and 80–100 (very high susceptibility). The indicators have their own weight definition processes.

### 3.1. *PhySFI Formulation*

The model formulation choice may fall on a product, a sum, or a combination of both possibilities. After more than 40 versions in the preliminary testing phase, with different formulations tested by the authors, the PhySFI was defined as a combination of a product of the slope, highlighted as the main flooding indicator, versus a sum of the other indicators.

Therefore, the slope was considered the fundamental aspect in terms of both the results observed in the literature review and the findings of our study. With this choice, even if a highly urbanized area is near a river course, the susceptibility to flooding can be low if the slope is high. In this study, as will be detailed in the normalized scale for the slope indicator (in the following sections), when the slope is greater than 8%, the slope indicator will be zero and so will the entire index. Equation (1) represents the final index formulation.

$$\text{PhySFI} = I_S^{E1} \times (c1 \times I_{\text{IMP}} + c2 \times I_{\text{PROX}} + c3 \times I_E)^{E2} \quad (1)$$

where:

- $E1$  and  $E2$  are weights assigned to indicators;
- $I_{\text{IMP}}$ —Imperviousness Indicator;
- $I_{\text{PROX}}$ —Proximity to Drainage Network Indicator;
- $I_E$ —Elevation Indicator;
- $I_S$ —Slope Indicator;

Note:  $E1 + E2 = 1$ ,  $C1 + C2 + C3 = 1$  and  $0 \leq \text{PhySFI} \leq 100$ . Figure 1 presents a summary of the PhySFI index.

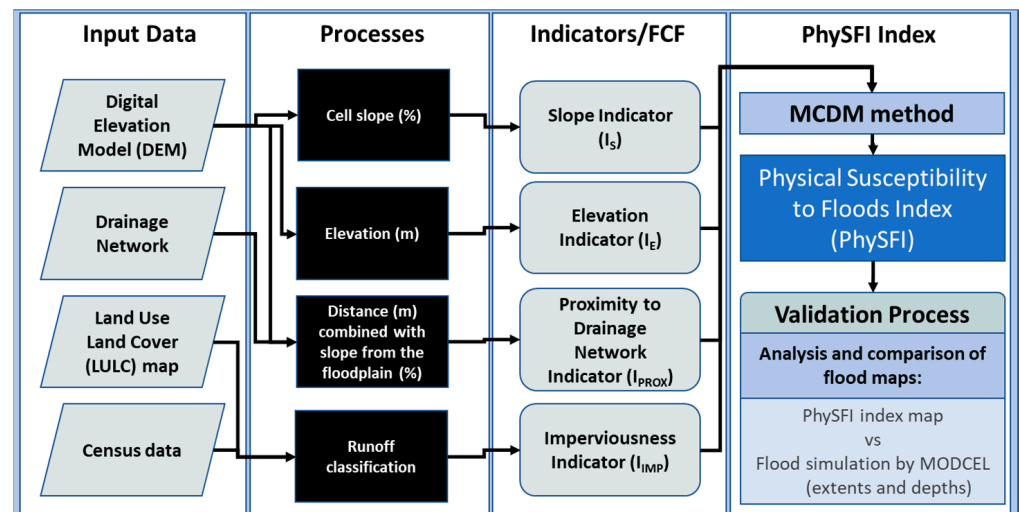


**Figure 1.** Horizontal grid resolution, given by the Brazilian National Institute for Space Research (INPE) [54], refined from SRTM raster [55]. The hydrography, land use and land cover files were provided by the city hall [52]. The population density in formal and slum areas was calculated using the Brazilian Institute of Geography and Statistics (IBGE) census data [56].

Three different units of interest were analyzed for PhySFI development and visualization as a way to provide useful data for different knowledge areas (Figure 2). The PhySFI can be presented in (1) raster format, (2) the census tract, a division for data collection that can change as the city grows, and (3) a statistical grid, a recent national strategy to make census data available in a permanent shape over time [57].

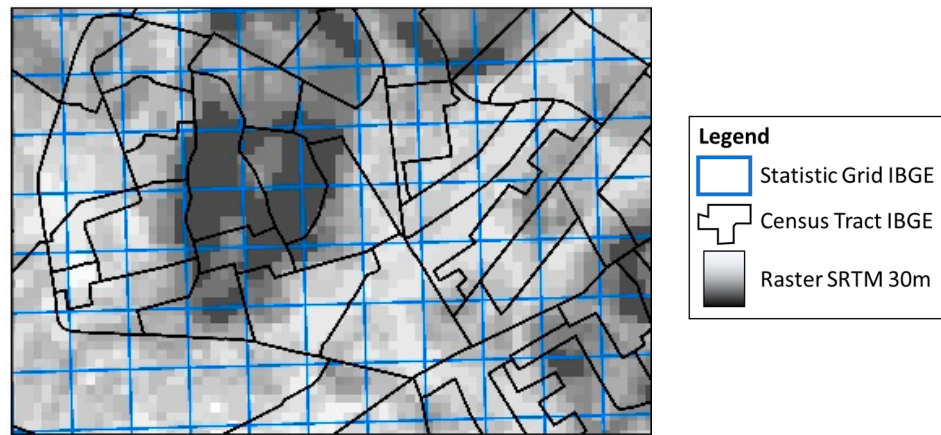


Figure 2. Different analysis units used in the PhySFI application.

### 3.2. Case Study: Rio de Janeiro City

With 6.7 million inhabitants occupying 1200 km<sup>2</sup> [56], the city of Rio de Janeiro presents extensive urbanized floodplains contrasting with mountains with forest fragments (Figure 2) and informal settlements. Flood events have been recorded in Rio since 1711, before the intense urbanization process that happened in the 20th century. Due to the city’s topography, large volumes of water flow downstream from the mountains, receiving increased runoff volumes from urbanized areas and finally reaching very low slope areas subjected to tidal influence. During the urbanization process, floodplains were intensely modified and occupied and extreme events and consequences became frequent.

The city is composed of more than 40 basins (Figure 3), excluding small islands. In general, continental watersheds are strongly marked by highly dense urban spots downstream, in contrast with vegetated protected mountains upstream. The average precipitation varies from 1200 to 2200 mm/year and the critical events are usually related to intense convective rainfall [55]. Some recent heavy rain events, such as the rains of January 1998 (272.8 mm/24 h) and April 2006 (252.8 mm/24 h), both recorded in the Tijuca massif, caused high damages to private and public assets.

Figure 4 presents the basins of more than 10 km<sup>2</sup>, highlighting their urban areas and population. The concept of “macrobasins” refers to administrative areas that join a set of near and similar watersheds.

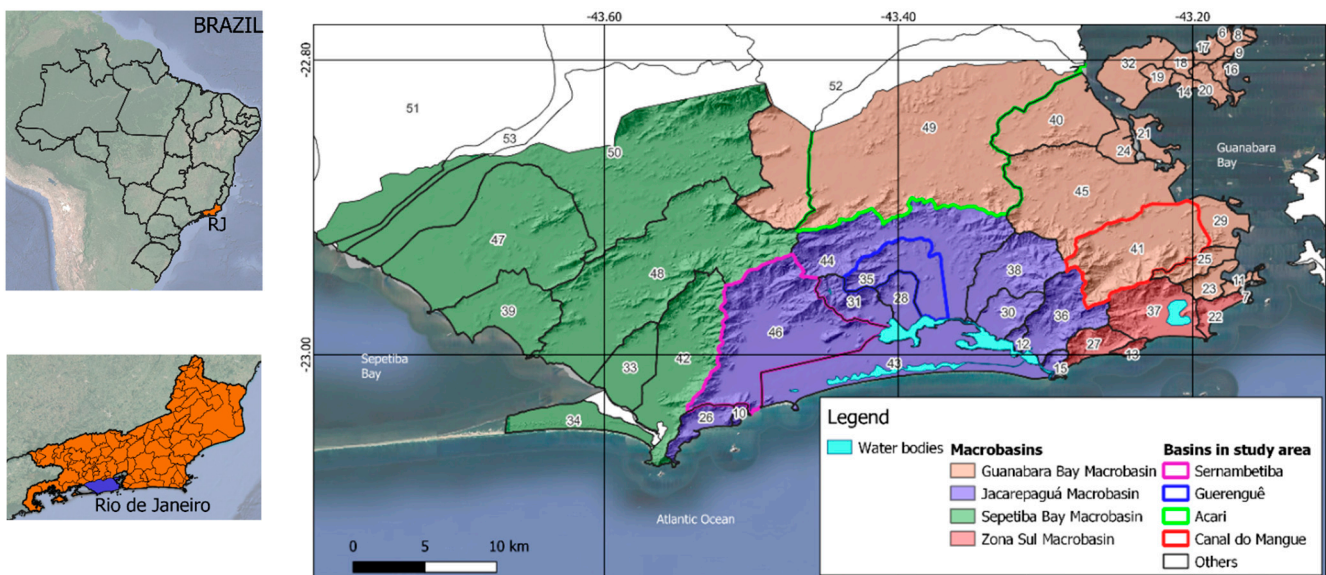


Figure 3. Basins of Rio de Janeiro City.

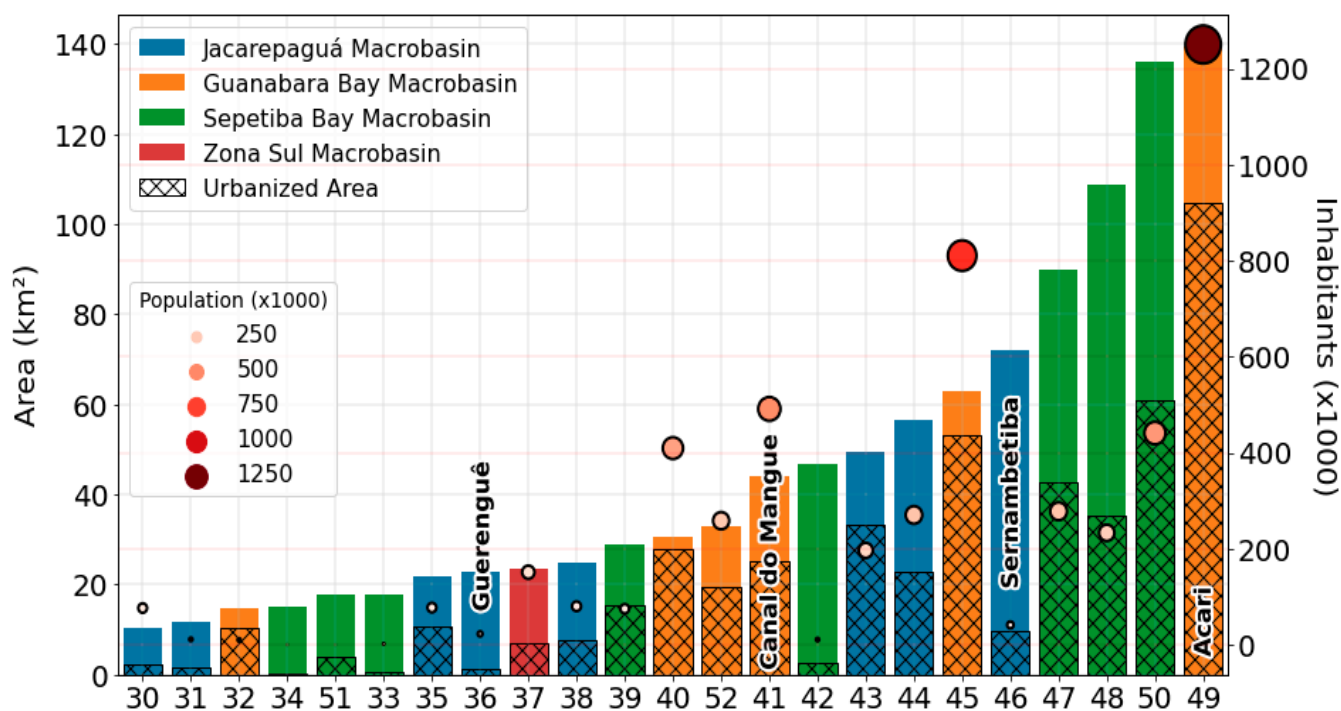


Figure 4. Area (km<sup>2</sup>) of basins that are bigger than 10 km<sup>2</sup> inside the study area. Basin codes according to Figure 3.

### 3.3. Formulation of the PhySFI Indicators

The Physical Susceptibility to Floods Index proposed in this study was based on only four floods, as previously defined, considering the physical interpretation and the content of previous studies [27–30,39,42]. In general, areas with low elevation and low slopes are more prone to flooding than others, which can be aggravated by land use characteristics and proximity to main channels. The indicators developed for the PhySFI index are presented in the following.

#### 3.3.1. I<sub>S</sub>—Slope Indicator

Slope classes and weights must be defined based on the phenomenon that one wants to model, e.g., whether different slope parameter choices will penalize flash floods or fluvial floods. In this study, the surface slopes are considered the most important parameters for flood susceptibility mapping when dealing with fluvial floods, since flat or mild areas are difficult to drain.

The normalized scale for this parameter was built by adapting an existing classification used by the Brazilian Agricultural Research Corporation (EMBRAPA) to the drainage efficiency expectations. Slope calculation was undertaken by using the maximum elevation difference between a pixel and its neighbors [58]. Table 1 presents the slope classification adopted in the present study.

Table 1. Slope indicator classification.

Slope for Drainage Categories	Slope Ranges (%)	Slope Indicator Value
Critical	≤1.5	100
Acceptable	1.5 < % ≤ 3.0	75
Adequate	3.0 < % ≤ 5.0	50
Good	5.0 < % ≤ 8.0	25
Very good	>8	0

### 3.3.2. $I_E$ —Elevation Indicator

Herein, the elevation (Figure 5) was classified based on the absolute values of terrain elevation and according to the longitudinal profile of river valleys in the study area (Figure 6) and the water depths obtained from the hydrodynamic modeling of four watersheds in the city to assess backwater effects. This approach catches the representation of flatter lowland areas and the potential tide effect on the final reaches of river courses and their floodplains.

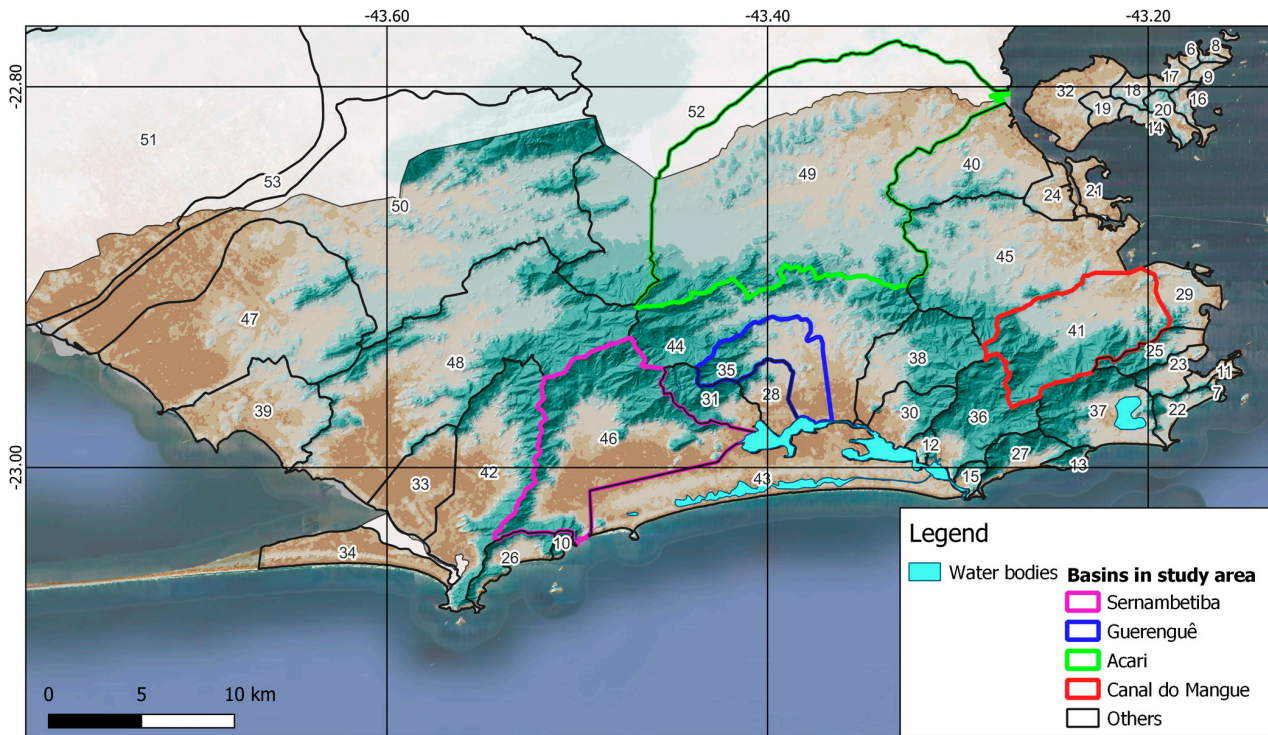


Figure 5. Rio de Janeiro elevation map.

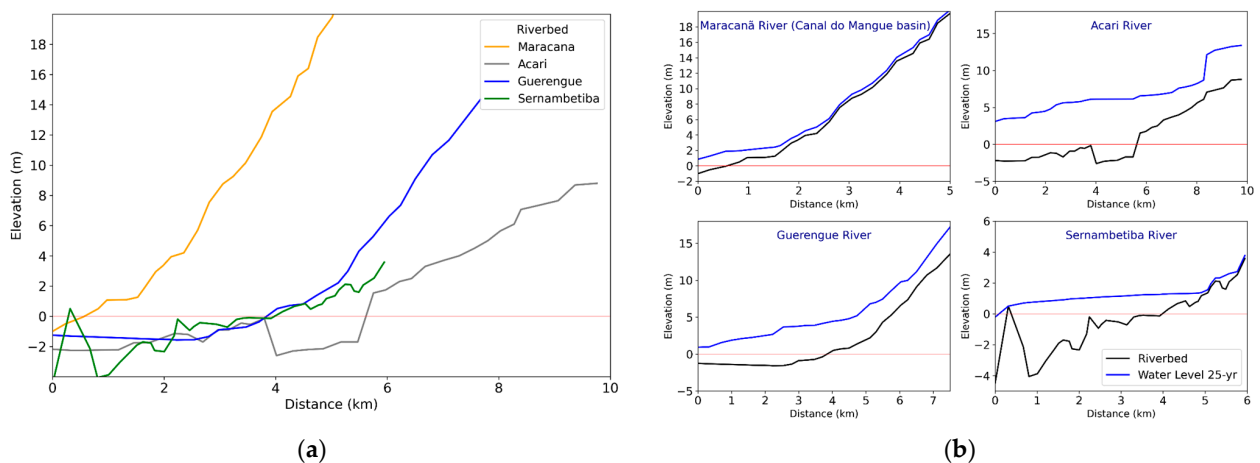


Figure 6. (a) Representative longitudinal profile of river valleys in the study area; (b) water heights resulting from the hydrodynamic modeling of the four basins' low stretches.

Considering river valley longitudinal profiles, it is possible to consider a higher tidal influence until the elevation of 5 m above mean sea level, in representative basins of the study area. In this sense, for Rio de Janeiro city, the elevation indicator was classified as presented in Table 2. The lower limit of 2 m was based on the municipal restriction for building licensing in potentially flooded areas.

**Table 2.** Elevation classification.

Elevation (m)	Elevation Indicator Value
≤2.0	100
2.0 < E ≤ 3.0	75
3.0 < E ≤ 4.0	50
4.0 < E ≤ 5.0	25
>5	0

**3.3.3. I<sub>PROX</sub>—Proximity to Drainage Network Indicator**

The I<sub>PROX</sub> formulation, a novelty proposed by the present study, comprises characteristics of the High Above the Nearest Drainage (HAND) model [59] and of the commonly used parameter “distance from river/drainage network” (DFDN). The I<sub>PROX</sub> analyzes the slope of the terrain and its distance concerning the nearest drainage line, aiming to represent the potential accesses of the surplus water overflowing the riverbanks. The sole consideration of distance parameters, such as DFDN, ignores valley zones where the transversal slope of floodplains increases considerably in short distances and flows are maintained mainly confined along the main channel. In a general conceptualization of a watershed, it is reasonable to consider that flat areas adjacent to the river are a proxy for flood-prone areas. The distances and rates given for this indicator in its normalized scale are presented in Table 3. Distance classes and indicator values were based on the basins’ scale of the study area (<140 sq.km) and can be adapted to other regions. An example of application in the study area is presented in Figure 7.

**Table 3.** Classes for the I<sub>PROX</sub> indicator.

Distance (D) from Main River Network (m)	Slope (%)				
	<1.5	1.5 < % < 3.0	3.0 < % < 5.0	5.0 < % < 8.0	5.0 < % < 8.0
≤100	100	100	75	50	25
100 < D ≤ 200	100	75	50	25	0
200 < D ≤ 300	75	50	25	0	0
300 < D ≤ 400	50	25	0	0	0
400 < D ≤ 500	25	0	0	0	0
>500	0	0	0	0	0

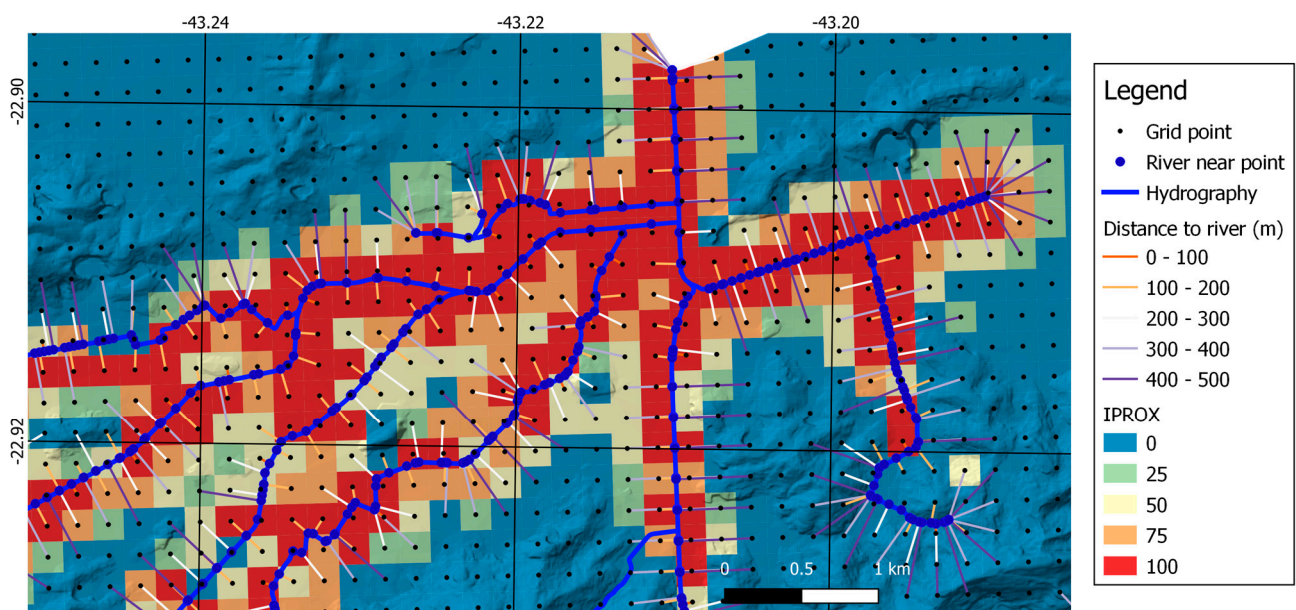


**Figure 7.** Example of I<sub>PROX</sub> indicator method application.

### 3.3.4. $I_{IMP}$ —Imperviousness Indicator

Land use modification appears as the largest flood intensification factor [6]. The urbanization process reduces infiltration and surface retention due to vegetation removal, the paving process and buildings' construction, increasing runoff and water accumulation above the surface [51]. The  $I_{IMP}$  indicator, based on LULC, is represented by the runoff coefficient value attributed to each land use. Table 4 presents the values assumed for land use classes for Rio de Janeiro city, adapted from a regional study [60]. In this case, the runoff coefficient is already a number between 0 and 100%.

**Table 4.** Runoff coefficients for  $I_{IMP}$ .

Land Use	Runoff Coefficient/ $I_{IMP}$ Values
Agricultural areas	20
Services and business areas	90
Education and health areas	70
Mineral exploitation areas	70
Recreational areas	40
Transportation areas	90
Non-built areas	30
Public infrastructure and institutional areas	70
Industrial areas	90
Wetlands	90
Exposed rocks	90
Canopy	10
Grass cover	20
Water bodies	100
<b>Residential Areas (formal and slums)</b>	
Low density	50
Medium density	70
High density	90

### 3.4. Climate Change Scenario Adaptation

Departing from the current indicators' values and weights, it is possible to create future scenarios for urban planning purposes. In this sense, a scenario was developed representing climate change impacts considering mean sea level rise and a shift in imperviousness indicator as a proxy for an increase in rainfall intensity. Considering that climate change is an important factor in the future performance of drainage systems, it is interesting to observe how the proposed index can react to this scenario.

Under the influence of mean sea level rising conditions, drainage pipes and channels may have their outflow section partially or completely drowned. Studies about sea level rise can present a significant variability in their results [61]. According to the Projected Sea Level Rise by the International Panel on Climate Change (IPCC), under Representative Carbon Pathway (RCP) 8.5 scenario, the mean sea level (MSL) rise could reach +0.4 m at the Brazilian coast in 2100 [62]. In a survey involving experts, a range between 0.45 and 1.65 m (5 to 95th percentiles) was suggested in Global Mean Sea Level (GMSL) rise, also in 2100 [61]. Due to the combination of storm surges, tides and waves, Extreme Sea Levels (ESLs) tend to increase the frequency of 100 year events, mainly in the tropics, including Rio de Janeiro city [63].

Considering this impact conservatively, an average value of +1.0 m was added in ranges to simulate the elevation indicator in the PhySFI Future Scenario, as presented in Table 5.

Based on historical data, the Rx1-day index (annual maximum 1-day precipitation) presents an increasing trend of approximately 10 mm/decade in Rio de Janeiro city [58,64,65]. Considering an average value of this index for the region as 110 mm in the current situation [64,65], the increase will be approximately 20% in 2040.

**Table 5.** Range values for elevation indicator in PhySFI Future Scenario for Rio de Janeiro city.

Elevation Ranges		Elevation Indicator Value
Current Situation	Future Scenario (Sea Level Rise 1 m)	
$\leq 2.0$	$\leq 3.0$	100
$2.0 < E \leq 3.0$	$3.0 < E \leq 4.0$	75
$3.0 < E \leq 4.0$	$4.0 < E \leq 5.0$	50
$4.0 < E \leq 5.0$	$5.0 < E \leq 6.0$	25
$> 5$	$> 6$	0

This rate was used as a reference for a chosen increase of plus 20 percent in all land use runoff values in the imperviousness indicator, representing a shift in runoff patterns promoted by rainfall increase. Table 6 presents the values of  $I_{IMP}$  in future scenarios with climate change impacts.

**Table 6.** Runoff coefficients for  $I_{IMP}$  in the current situation and future scenario of 2040.

Land Use	$I_{IMP}$ Values	
	Current Situation	Future Scenario
Agricultural areas	20	24
Services and business areas	90	100
Education and health areas	70	84
Mineral exploitation areas	70	84
Recreational areas	40	48
Transportation areas	90	100
Non-built areas	30	100
Public infrastructure and institutional areas	70	84
Industrial areas	90	36
Wetlands	90	100
Exposed rocks	90	100
Canopy	10	12
Grass cover	20	18
Water bodies	100	100
Residential Areas (formal and slums)		
Low density	50	60
Medium density	70	84
High density	90	100

#### 4. Results

Four basins within the study area were hydrologically and hydrodynamically modeled for a 25 year rainfall event [66–70], using MODCEL to map significant floods and compare the real results with the expected susceptibility to flooding, as presented in the following.

##### 4.1. Canal de Sernambetiba Basin

Formed by an extensive lowland area, with a series of artificial desiccation channels and low altimetry levels, the middle stretch of the Canal de Sernambetiba basin suffers from floods of large extensions with a predominance of water depths between 0.30 and 0.75 m. Despite a series of human interventions in the drainage network, the region still maintains natural characteristics and its current occupation is insignificant compared to the rest of the city [69]. In this case, PhySFI was able to satisfactorily represent areas susceptible to flooding once FHS and FSM had highlighted the same areas, as presented in Figure 8.

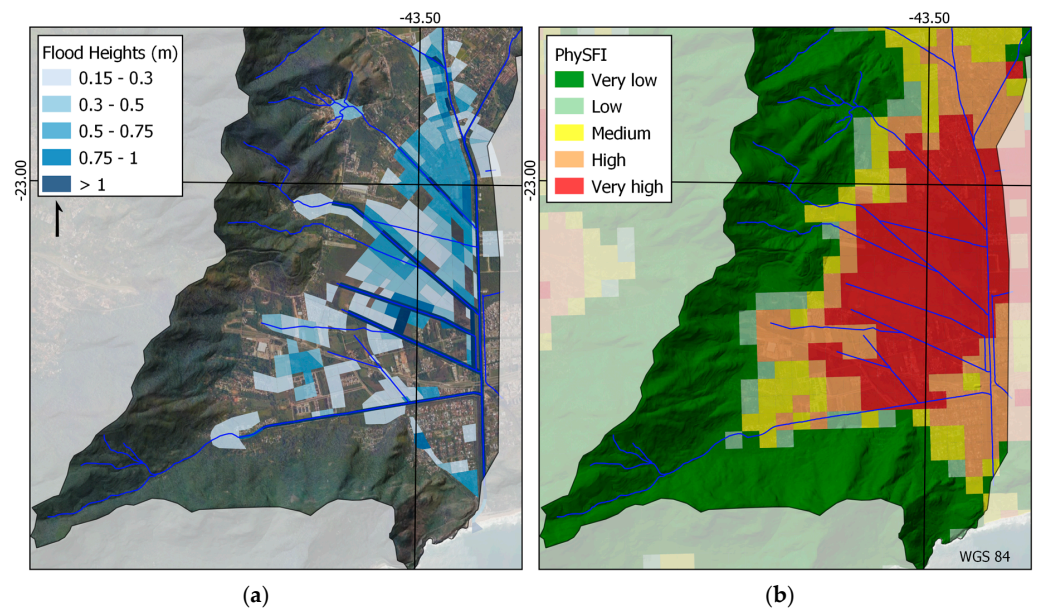


**Figure 8.** Comparison in Canal de Sernambetiba basin: (a) hydrodynamic 25 year results and (b) PhySFI results.

4.2. *Guerenguê Basin*

The middle stretch of the basin, with a predominance of water depths exceeding 1 m in height, was identified by the index to be within the highest range of susceptibility of the physical environment to flooding. The low stretch was identified as highly susceptible. However, high flood heights are not verified in the simulation for a 25 year return period event due to the presence of marginal dikes in this region, preventing the overflow of water in the gutter for the simulated rain [68]. However, the PhySFI results for this region indicate the residual risk for the events simulated above, as presented in Figure 9.

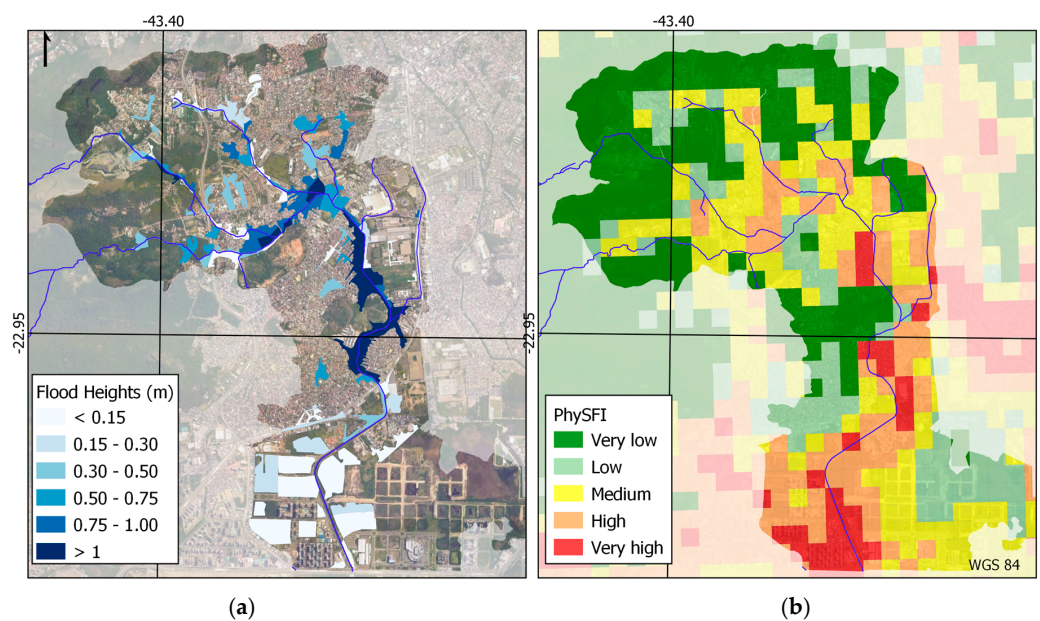


**Figure 9.** Comparison in Guerenguê basin: (a) hydrodynamic 25 year results and (b) PhySFI results.

4.3. *Canal Do Mangue Basin*

The Canal do Mangue basin is characterized by a high degree of soil waterproofing, embankments in its lower part, high channeling and different interventions in rivers. The PhySFI results revealed problematic regions, such as Bandeira, Niterói and Varnhagem

squares (numbers 1, 3 and 4 in Figure 10), which currently have reservoirs for flood control and others with recurring flood problems such as Saens Peña and Afonso Pena squares (numbers 6 and 2). Areas downstream of the Praça da Bandeira square (1) presented high susceptibility values, but they were not confirmed in hydrodynamic modeling. In practice, the railway works as a barrier for runoff and retains volume upstream [70].

In general, water depths are spatialized over the watershed and floods are highly conditioned by drainage network capacity and maintenance.

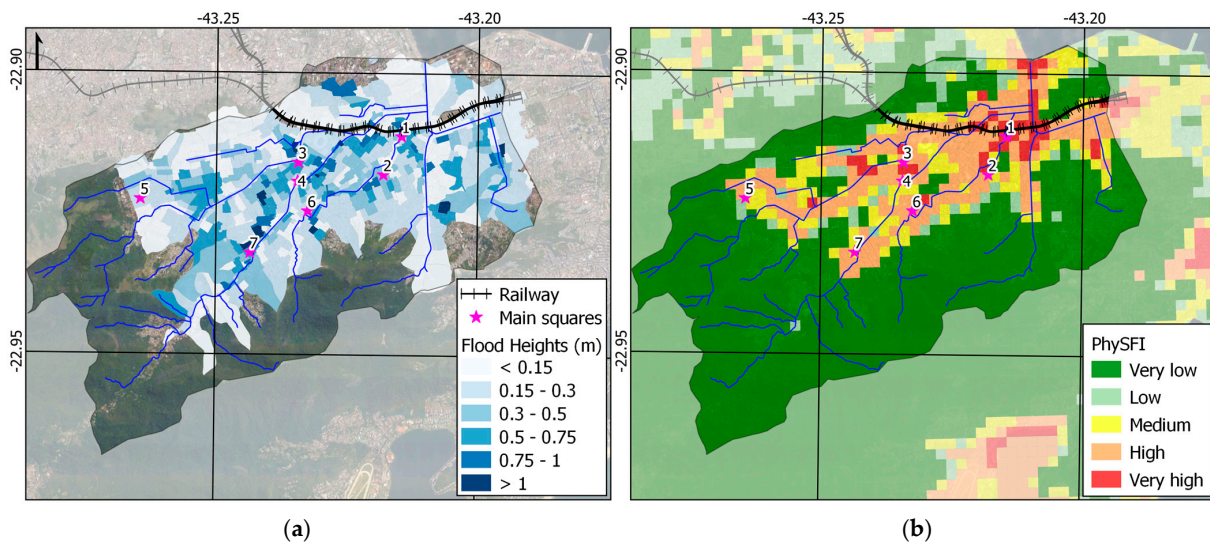


**Figure 10.** Comparison in Canal do Mangue basin: (a) hydrodynamic 25 yr results and (b) PhySFI results.

#### 4.4. Acari Basin

For the Acari River basin (Figure 11), the regions highlighted by the index did not show satisfactory correspondence concerning the flood spots resulting from the mathematical modeling. The basin is highly modified and waterproofed, including several inadequate works, which restrict flows (strangulated passages under bridges, bridges with excess pillars in the gutter, galleries with singularities and narrowing sections) and aggravate flooding in several regions of the watershed [8,9,67].

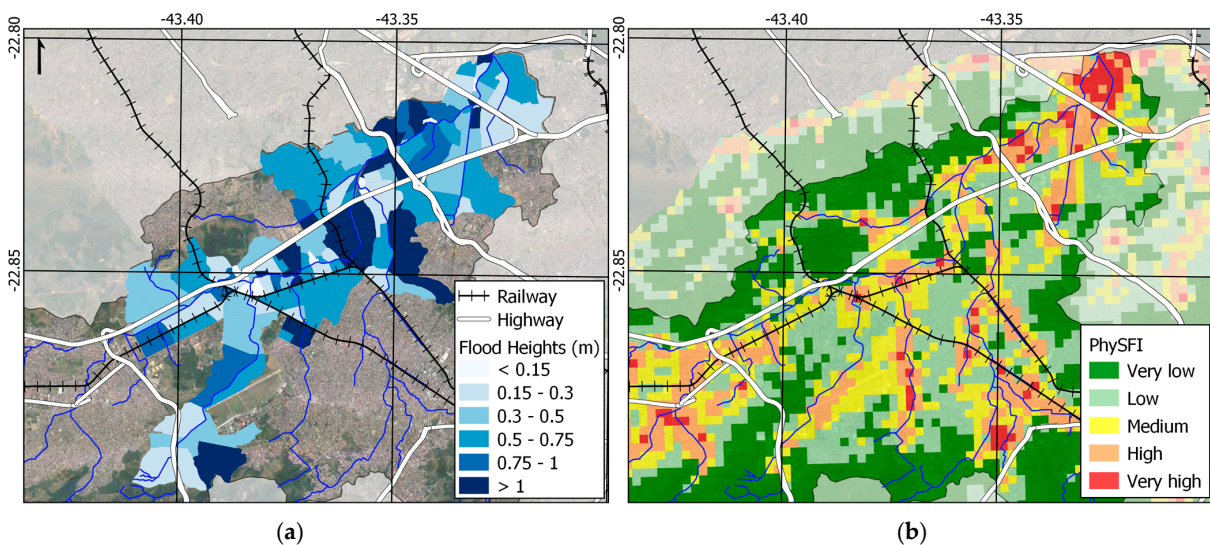


**Figure 11.** Comparison in Acari basin: (a) hydrodynamic 25 year results and (b) PhySFI results.

#### 4.5. PhySFI Final Formulation

After a set of testing applications, the PhySFI final formulation, including an optimized choice for the weights, is presented in Equation (2). Figure 12 shows the spatial results for each indicator.

$$\text{PhySFI} = I_S^{0.25} \times (0.4 \times I_{\text{IMP}} + 0.4 \times I_{\text{PROX}} + 0.2 \times I_E)^{0.75} \quad (2)$$

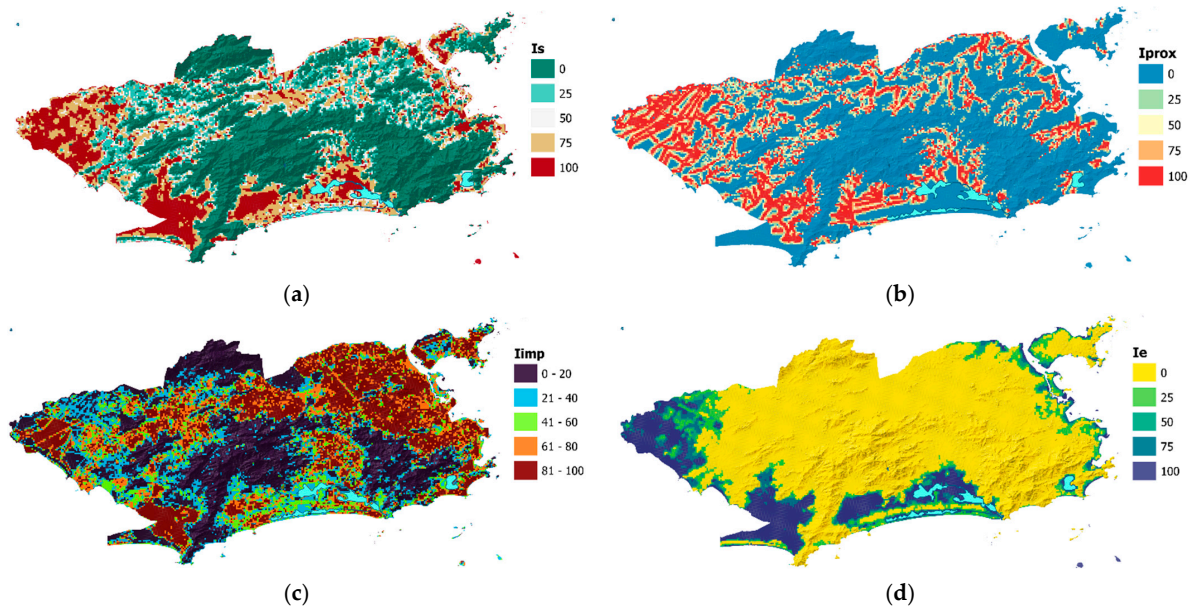


Figure 12. Spatial results for each of the PhySFI indicators: (a) slope; (b) proximity; (c) imperviousness; (d) elevation.

A more detailed result for the PhySFI application in Rio de Janeiro city for the current scenario using the statistical grid is presented in Figure 13. The obtained spatialized results for different basic spatial units appear in Figure 14.

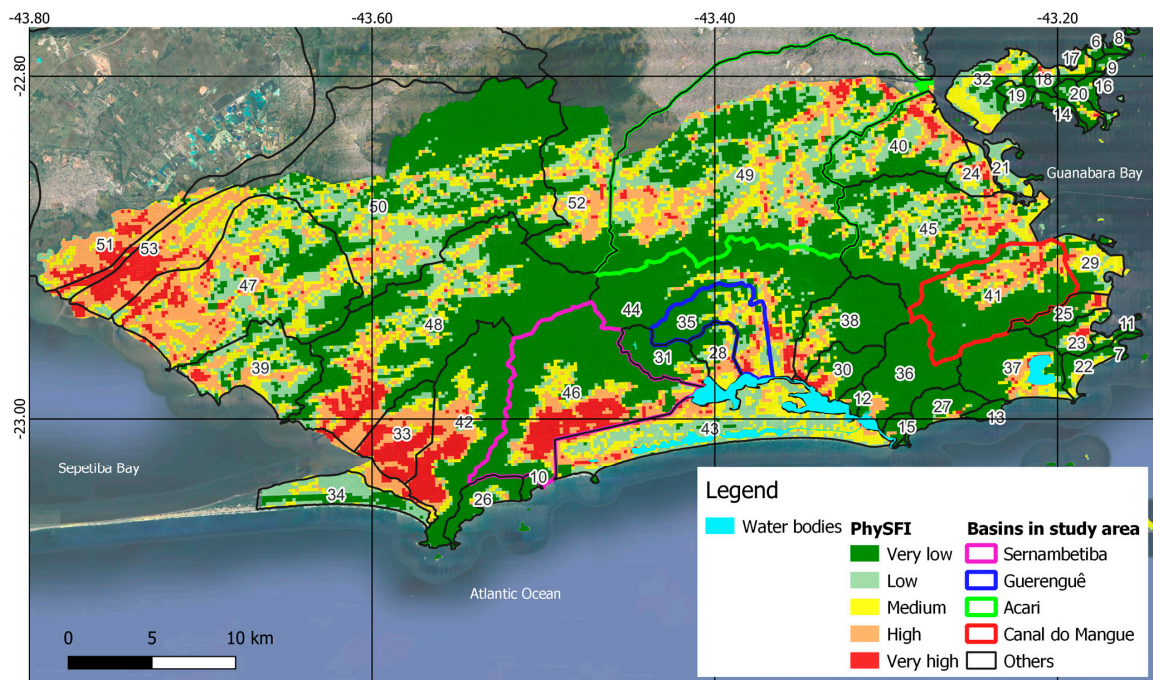
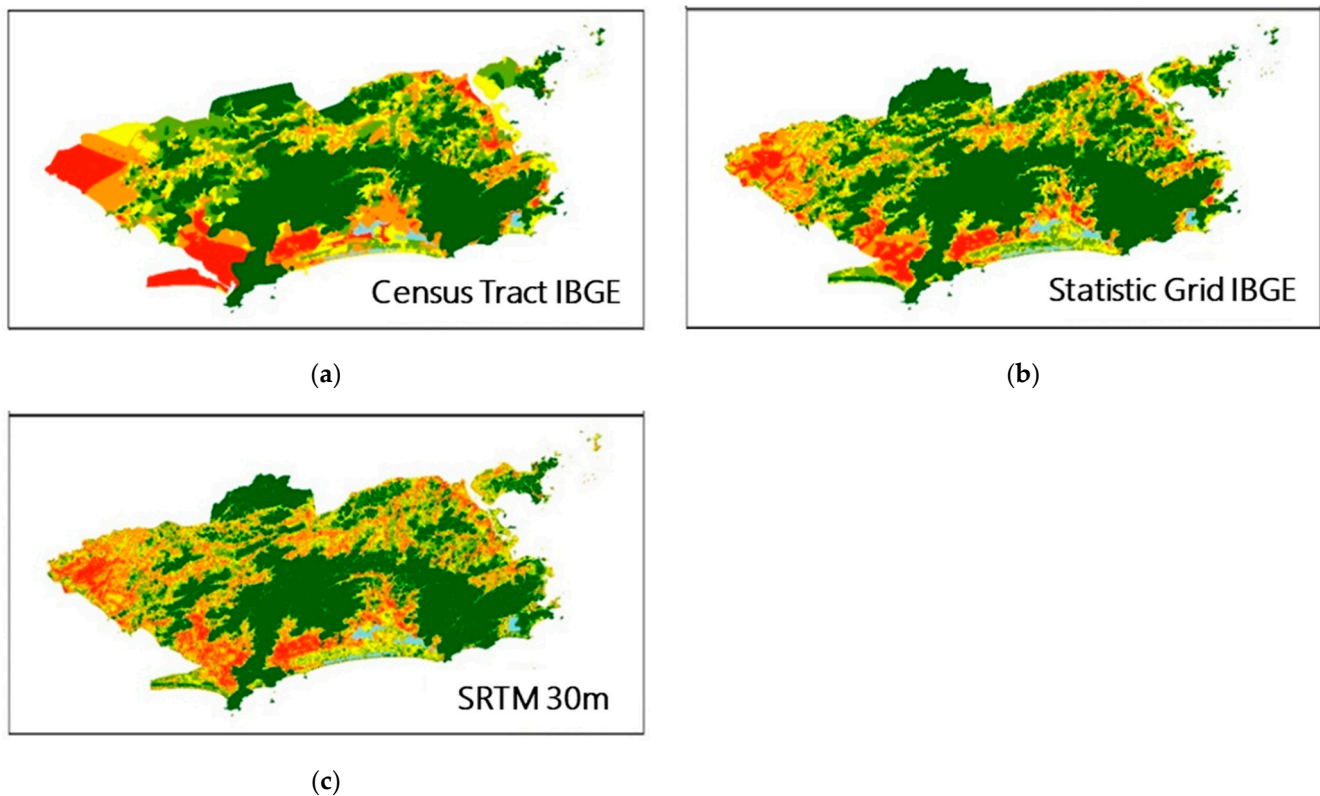


Figure 13. Final PhySFI result for the city of Rio de Janeiro.



**Figure 14.** PhySFI results for different study units: (a) Census Tract IBGE (2010); (b) Statistic Grid IBGE (2016); (c) SRTM 30 m raster pixel.

#### 4.6. Overview

The PhySFI results obtained for the city of Rio de Janeiro in the current situation have shown a greater coherence in less urbanized watersheds, such as Sernambetiba and Guerenguê Rivers—in these cases, the original watershed is less modified by urban and hydraulic structures, which makes the susceptibility results closer to those of the hydrodynamic modeling. It was possible, for example, to confirm the high susceptibility of their floodplains. Higher levels of formal urbanization, such as those found in the Canal do Mangue, led the index to show high values for large extents of the watershed. These areas were partially verified in the hydrodynamic modeling; however, some areas indicated by the PhySFI are not flooded in the current situation, because flood control reservoirs are now located in these areas.

In the Acari River basin, which is a highly disordered urban catchment, the index presented regions with high and very high susceptibility that differed from the hydrodynamic modeling results, due to a set of hydraulic works, low bridges, the insufficient capacity of storm drains, etc. These features promote floods in unexpected parts of the basin. However, the information offered by the index results can show that the residual risks still exist (even if areas are not flooded because of existing flood protections, or because upstream reaches are flooded due to the system conveyance incapacity).

#### 4.7. Climate Change Scenario

The climate change impacts simulated affected the basins in the study area (Figure 15) differently depending on the urbanization pattern of each watershed and the proximity to the coastal areas.

Analyzing the results according to macrobasins, Guanabara Bay concentrates the majority of people in High or Very High susceptibility to flood categories, corresponding to almost 100 thousand inhabitants, as presented in Figure 16a.

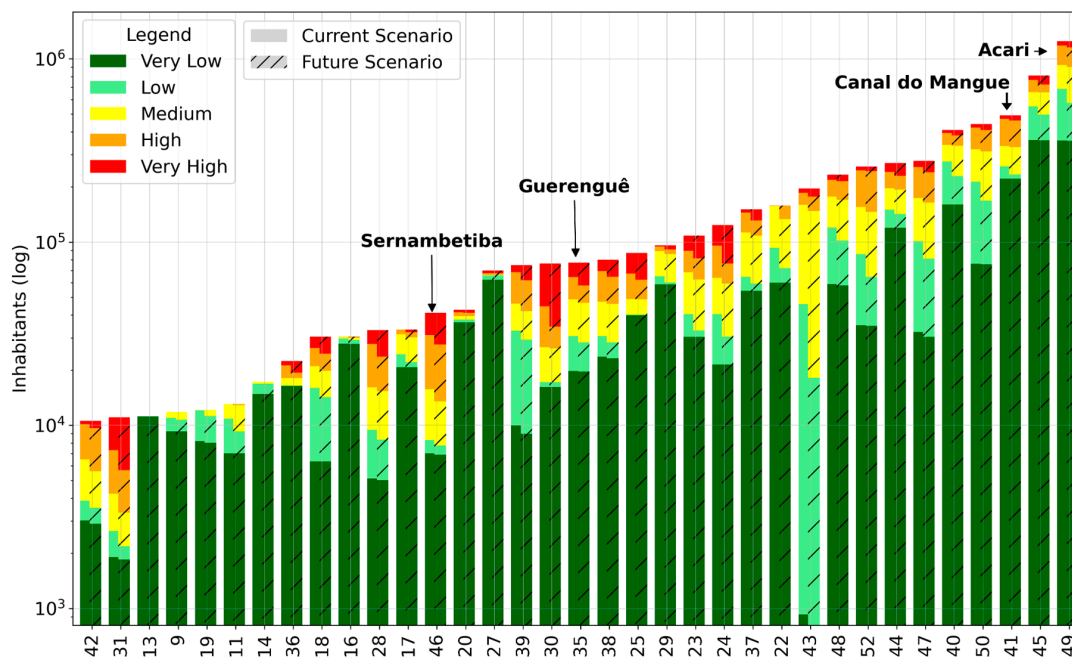


**Figure 15.** PhysSFI results in the current situation and future scenario for all the watersheds in the study area. Basin code according Figure 1.

In all macrobasins, people living in Very Low susceptibility areas are almost unaffected, with the exception of Sepetiba Bay. On the other hand, the number of people living in urbanized flood plains near the coast is impacted in all cases.

Considering the results in the current scenario as a reference, about 26% of Rio de Janeiro’s city population lives in areas considered to be at high or very high susceptibility to flooding, which corresponds to 21% of the city territory (Figure 16b). In an overview of the city’s susceptibility results in the future scenario, almost 241,000 inhabitants will live in areas with very high susceptibility to flood, which means an increase of 58% in this index class and 4% of the overall population of the municipality.

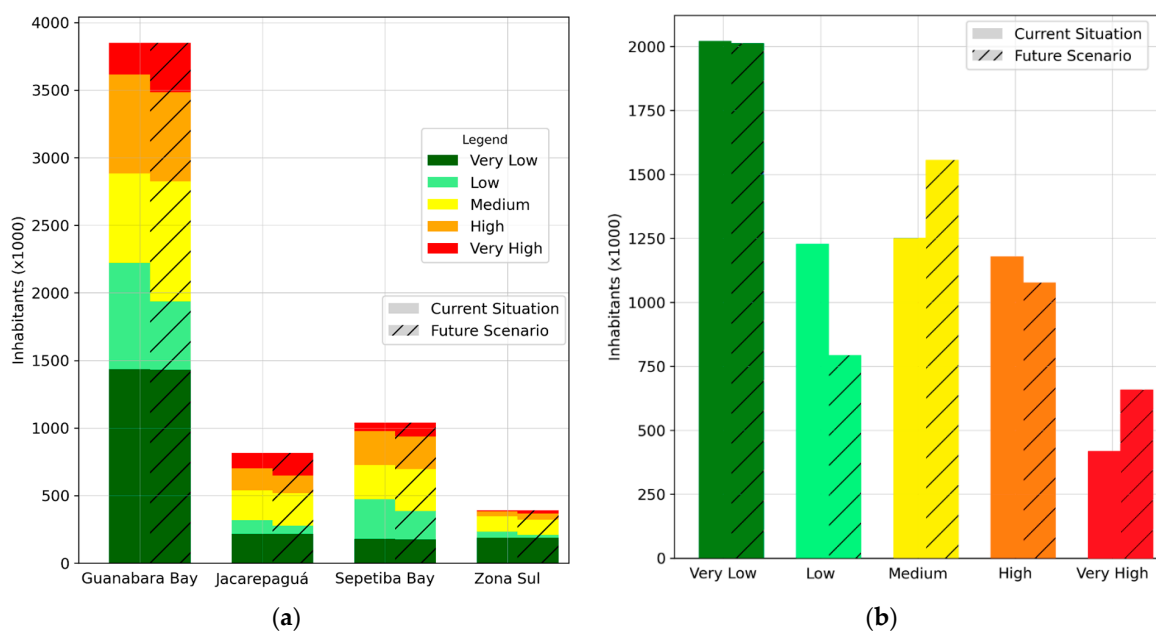


**Figure 16.** PhysSFI results in the current situation and future scenario for: (a) the macro basins of the study area; (b) Rio de Janeiro city.

## 5. Conclusions

The main goal of the present study was to develop a simple and robust method to measure the physical susceptibility to floods of a certain territory, using widely available input data. This method corresponds to the PhySFI tool, which can also offer easy replication to other watersheds. All the steps taken in the index development procedure were based on choices that allow their reproducibility for other cases. All data are relatively easy to obtain and geospatial tools are available in open and free GIS software.

The PhySFI results obtained for four modeled basins suggested a better relationship between flood susceptibility and flood hazard in the less urbanized catchments, where the original physical setup is still the strongest factor driving the phenomenon. The built environment may introduce changes in runoff patterns, creating new flooding areas while protecting the original old ones. In this sense, in more rural areas PhySFI has greater potential to subsidize land use planning. On the other hand, in highly urbanized areas, PhySFI tends to highlight areas that still can be threatened by residual risks—which can be something important to guide decisions on compacting (or not) a certain region. In this latter case, the PhySFI results can be seen as a flood memory aid for decision makers.

Therefore, the PhySFI can be used as a tool for flood susceptibility assessments intended to support urban planning and development. In large and/or non-coastal basins, the elevation indicator can be neglected by using a zero weight. In general, all indicators may be adjusted for the applied region, considering existing data and geographical conditions and also including changes in their classes and weights. Further steps in this research could benefit from a set of different applications, such as using urban watersheds with different characteristics in order to assess the indicator's sensitivity and map eventual gaps in the formulation.

Flood susceptibility analysis comprises a portion of the Flood Risk Management approach and preferably should be followed by hazard, risk and resilience analyses.

**Author Contributions:** Conceptualization, M.M., O.R., A.B.F. and F.M.; methodology, M.M., O.R., A.B.F. and F.M.; software, F.M. and A.B.F.; validation, M.M., O.R. and A.N.H.; formal analysis, F.M.; investigation, F.M.; resources, M.M.; data curation, F.M.; writing—original draft preparation, F.M.; writing—review and editing, F.M., B.B.F.d.C. and M.N.; visualization, F.M., B.B.F.d.C. and M.N.; supervision, M.M. and O.R.; project administration, M.M. and O.R.; funding acquisition, A.N.H. All authors have read and agreed to the published version of the manuscript.

**Funding:** This work was supported by the Coordenação de Aperfeiçoamento de Pessoal de Nível Superior-Brazil (CAPES), Finance Code 001; Conselho Nacional de Desenvolvimento Científico e Tecnológico – Brasil (CNPq) under Grant [303862/2020-3].

**Institutional Review Board Statement:** Not applicable.

**Informed Consent Statement:** Not applicable.

**Data Availability Statement:** Not applicable.

**Acknowledgments:** The authors would like to acknowledge Conselho Nacional de Desenvolvimento Científico e Tecnológico (CNPq), and Fundação Carlos Chagas Filho de Amparo à Pesquisa do Estado do Rio de Janeiro (FAPERJ), which helped in the development of this work. The authors also would like to acknowledge the UNESCO Chair for Urban Drainage in Regions of Coastal Lowlands, at Universidade Federal do Rio de Janeiro, which houses this research.

**Conflicts of Interest:** The authors declare no conflict of interest.

## References

1. Merz, B.; Kreibich, H.; Schwarze, R.; Thielen, A. Review article “assessment of economic flood damage”. *Nat. Hazards Earth Syst. Sci.* **2010**, *10*, 1697–1724. [CrossRef]
2. Whitfield, P. Floods in future climates: A review. *J. Flood Risk Manag.* **2012**, *5*, 336–365. [CrossRef]
3. CRED. EM-DAT Public Database [WWW Document]. Centre for Research on the Epidemiology of Disasters. 2022. Available online: <https://reliefweb.int/> (accessed on 4 May 2023).

4. Wannous, C.; Velasquez, G. United Nations Office for Disaster Risk Reduction (UNISDR)—UNISDR’s Contribution to Science and Technology for Disaster Risk Reduction and the Role of the International Consortium on Landslides (ICL). *Adv. Cult. Living Landslides* **2017**, *2017*, 109–115. [[CrossRef](#)]
5. World Bank. Urban Population (% of Total Population) [WWW Document]. United Nations Population Division. World Urbanization Prospects: 2018 Revision. 2022. Available online: <https://data.worldbank.org/indicator/SP.URB.TOTL.IN.ZS> (accessed on 10 May 2023).
6. Scheuler, T.R. *Controlling Urban Runoff: A Practical Manual for Planning and Designing Urban BMPs*; Metropolitan Washington Council of Governments: Washington, DC, USA, 1987.
7. Hooke, J. Variations in flood magnitude–effect relations and the implications for flood risk assessment and river management. *Geomorphology* **2015**, *251*, 91–107. [[CrossRef](#)]
8. De Oliveira, A.K.B.; Battemarco, B.P.; Barbaro, G.; Gomes, M.V.R.; Cabral, F.M.; Bezerra, R.d.O.P.; Rutigliani, V.D.A.; Lourenço, I.B.; Machado, R.K.; Rezende, O.M.; et al. Evaluating the Role of Urban Drainage Flaws in Triggering Cascading Effects on Critical Infrastructure, Affecting Urban Resilience. *Infrastructures* **2022**, *7*, 153. [[CrossRef](#)]
9. Guimarães, L.; Battemarco, B.; Oliveira, A.; Miguez, M. A new approach to assess cascading effects of urban floods. *Energy Rep.* **2021**, *7*, 8357–8367. [[CrossRef](#)]
10. Sayers, P.; Li, Y.; Galloway, G.; Penning-Rowsell, E.; Shen, F.; Kang, W.; Yiwei, C.; Le Quesne, T. *Flood Risk Management: A Strategic Approach*; Asian Development Bank: Metro Manila, Philippines, 2013; ISBN 9789230011598.
11. Correia, F.N.; Da Graça Saraiva, M.; Nunes, F.; Silva, D.A.; Ramos, I. Floodplain Management in Urban Developing Areas. Part I. Urban Growth Scenarios and Land-Use Controls, Water Resources Management. *Water Resour. Manag.* **1999**, *13*, 1–21. [[CrossRef](#)]
12. Shinde, S.; Pande, C.B.; Barai, V.N.; Gorantiwar, S.D.; Atre, A.A. Flood impact and damage assessment based on the sentinel-1 SAR data using google earth engine. In *Climate Change Impacts on Natural Resources, Ecosystems and Agricultural Systems*; Springer International Publishing: Cham, Switzerland, 2023; pp. 483–502.
13. Mudashiru, R.B.; Sabtu, N.; Abustan, I. Quantitative and semi-quantitative methods in flood hazard/susceptibility mapping: A review. *Arab. J. Geosci.* **2021**, *14*, 941. [[CrossRef](#)]
14. Nguyen, N.-M.; Bahramloo, R.; Sadeghian, J.; Sepehri, M.; Nazaripouya, H.; Dinh, V.N.; Ghahramani, A.; Talebi, A.; Elkhachy, I.; Pande, C.B.; et al. Ranking Sub-Watersheds for Flood Hazard Mapping: A Multi-Criteria Decision-Making Approach. *Water* **2023**, *15*, 2128. [[CrossRef](#)]
15. Climate Change Adaptation Strategy for the City of Rio de Janeiro. Rio de Janeiro, RJ. 2016. Available online: <http://www.rio.rj.gov.br/dlstatic/10112/9857523/4243336/ClimateChangeAdaptationStrategyfortheCityofRiodeJaneiro.pdf> (accessed on 15 April 2023).
16. Kobiyama, M.; Goerl, R.F. Quantitative method to distinguish flood and flash flood as disasters. *SUISUI Hydrol. Res. Lett.* **2007**, *1*, 11–14. [[CrossRef](#)]
17. Silva, G.; Miguez, M.; Di Gregorio, L.T.; Veról, A.P. Vulnerability Index—Application and suitability of different methodologies applied to the municipality of Cuiabá, Mato Grosso-Brazil. *E3S Web Conf.* **2016**, *7*, 08013. [[CrossRef](#)]
18. Rezende, O.M.; Miranda, F.M.; Haddad, A.N.; Miguez, M.G. A Framework to Evaluate Urban Flood Resilience of Design Alternatives for Flood Defence Considering Future Adverse Scenarios. *Water* **2019**, *11*, 1485. [[CrossRef](#)]
19. Bertilsson, L.; Wiklund, K.; de Moura Tebaldi, I.; Rezende, O.M.; Veról, A.P.; Miguez, M.G. Urban flood resilience—A multi-criteria index to integrate flood resilience into urban planning. *J. Hydrol.* **2019**, *573*, 970–982. [[CrossRef](#)]
20. European Parliament. Directive 2007/60/EC of the European Parliament and of the Council of 23 October 2007 on the assessment and management of flood risks (Text with EEA relevance), 6.11.2007. *Off. J. Eur. Union* **2007**, *L288*, 27–34.
21. Merz, R.; Blöschl, G. A process typology of regional floods. *Water Resour. Res.* **2003**, *39*, 1340. [[CrossRef](#)]
22. Cloutier, C.-A.; Buffin-Bélanger, T.; Larocque, M. Controls of groundwater floodwave propagation in a gravelly floodplain. *J. Hydrol.* **2014**, *511*, 423–431. [[CrossRef](#)]
23. Zain, A.; Legono, D.; Rahardjo, A.P.; Jayadi, R. Review on Co-factors Triggering Flash Flood Occurrences in Indonesian Small Catchments. *IOP Conf. Ser. Earth Environ. Sci.* **2021**, *930*, 012087. [[CrossRef](#)]
24. Correia, F.N.; Rego, F.C.; Saraiva, M.D.G.; Ramos, I. Coupling GIS with Hydrologic and Hydraulic Flood Modelling. *Water Resour. Manag.* **1998**, *12*, 229–249. [[CrossRef](#)]
25. Malczewski, J. GIS-based multicriteria decision analysis: A survey of the literature. *Int. J. Geogr. Inf. Sci.* **2006**, *20*, 703–726. [[CrossRef](#)]
26. Jacinto, R.; Grosso, N.; Reis, E.; Dias, L.; Santos, F.D.; Garrett, P. Continental Portuguese Territory Flood Susceptibility Index—Contribution to a vulnerability index. *Nat. Hazards Earth Syst. Sci.* **2015**, *15*, 1907–1919. [[CrossRef](#)]
27. Kazakis, N.; Kougiyas, I.; Patsialis, T. Assessment of flood hazard areas at a regional scale using an index-based approach and Analytical Hierarchy Process: Application in Rhodope–Evros region, Greece. *Sci. Total. Environ.* **2015**, *538*, 555–563. [[CrossRef](#)] [[PubMed](#)]
28. Tehrany, M.S.; Pradhan, B.; Jebur, M.N. Spatial prediction of flood susceptible areas using rule based decision tree (DT) and a novel ensemble bivariate and multivariate statistical models in GIS. *J. Hydrol.* **2013**, *504*, 69–79. [[CrossRef](#)]
29. Tehrany, M.S.; Lee, M.-J.; Pradhan, B.; Jebur, M.N.; Lee, S. Flood susceptibility mapping using integrated bivariate and multivariate statistical models. *Environ. Earth Sci.* **2014**, *72*, 4001–4015. [[CrossRef](#)]

30. Tehrany, M.S.; Pradhan, B.; Mansor, S.; Ahmad, N. Flood susceptibility assessment using GIS-based support vector machine model with different kernel types. *Catena* **2015**, *125*, 91–101. [[CrossRef](#)]
31. Cian, F.; Marconcini, M.; Ceccato, P. Normalized Difference Flood Index for rapid flood mapping: Taking advantage of EO big data Flood mapping. *Remote Sens. Environ.* **2018**, *209*, 712–730. [[CrossRef](#)]
32. Bhattacharya, B.; Islam, T.; Masud, S.; Suman, A.; Solomatine, D. The use of a flood index to characterise flooding in the north-eastern region of Bangladesh. In Proceedings of the 3rd European Conference on Flood Risk Management, Lyon, France, 17–21 October 2016; Volume 10003, pp. 4–8.
33. Zonensein, J.; Gomes Miguez, M.; Cesar, F.; Mascarenhas, B. Flood Risk Index as an Urban Management Tool. In Proceedings of the 11th International Conference on Urban Drainage, Edinburgh, UK, 31 August–5 September 2008.
34. Zaharia, L.; Costache, R.; Prăvălie, R.; Ioana-Toroimac, G. Mapping flood and flooding potential indices: A methodological approach to identifying areas susceptible to flood and flooding risk. Case study: The Prahova catchment (Romania). *Front. Earth Sci.* **2017**, *11*, 229–247. [[CrossRef](#)]
35. Miguez, M.G.; Raupp, I.P.; Veról, A.P. An integrated quantitative framework to support design of resilient alternatives to manage urban flood risks. *J. Flood Risk Manag.* **2018**, *12*, 1–13. [[CrossRef](#)]
36. Tebaldi, I.; Miguez, M.; Battemarco, B.O.; Rezende, O.M.; Veról, A.P. Resilience index for flood events: Joana river catchment study case. In Proceedings of the XXI Simpósio Brasileiro de Recursos Hídricos, Rio de Janeiro, Brazil, 22 November 2015; pp. 1–8.
37. Batica, J.; Gourbesville, P. Flood Resilience Index-Methodology and Application Flood Resilience Index-Methodology and Application. 2014. Available online: [https://academicworks.cuny.edu/cc\\_conf\\_hic/433Discoveradditionalworksat:https://academicworks.cuny.edu](https://academicworks.cuny.edu/cc_conf_hic/433Discoveradditionalworksat:https://academicworks.cuny.edu) (accessed on 11 April 2023).
38. Schwarz, I.; Ziegelaar, M.; Kelly, M.; Watkins, A.B.; Kuleshov, Y. Flood Resilience Assessment and Mapping: A Case Study from Australia’s Hawkesbury-Nepean Catchment. *Climate* **2023**, *11*, 39. [[CrossRef](#)]
39. Mahmoud, S.H.; Gan, T.Y. Multi-criteria approach to develop flood susceptibility maps in arid regions of Middle East. *J. Clean. Prod.* **2018**, *196*, 216–229. [[CrossRef](#)]
40. Campolo, M.; Soldati, A.; Andreussi, P. Artificial neural network approach to flood forecasting in the River Arno. *Hydrol. Sci. J.* **2003**, *48*, 381–398. [[CrossRef](#)]
41. Pham, B.T.; Avand, M.; Janizadeh, S.; Van Phong, T.; Al-Ansari, N.; Ho, L.S.; Das, S.; Van Le, H.; Amini, A.; Bozchaloei, S.K.; et al. GIS Based Hybrid Computational Approaches for Flash Flood Susceptibility Assessment. *Water* **2020**, *12*, 683. [[CrossRef](#)]
42. Rahmati, O.; Zeinivand, H.; Besharat, M. Flood hazard zoning in Yasooj region, Iran, using GIS and multi-criteria decision analysis. *Geomat. Nat. Hazards Risk* **2016**, *7*, 1000–1017. [[CrossRef](#)]
43. Toye, J. Poverty reduction. *Dev. Pract.* **2007**, *17*, 505–510. [[CrossRef](#)]
44. Viessman, W., Jr. Integrated water management. *J. Contemp. Water Res. Educ.* **2011**, *106*, 2. [[CrossRef](#)]
45. Pörtner, H.-O.; Roberts, D.C.; Tignor, M.; Poloczanska, E.S.; Mintenbeck, K.; Alegria, A.; Craig, M.; Langsdorf, S.; Löschke, S.; Möller, V.; et al. IPCC, 2022: Climate Change 2022: Impacts, Adaptation, and Vulnerability. In *Contribution of Working Group II to the Sixth Assessment Report of the Intergovernmental Panel on Climate Change*; IPCC: Cambridge, UK; New York, NY, USA, 2022.
46. Saito, N. Challenges for adapting Bangkok’s flood management systems to climate change. *Urban Clim.* **2014**, *9*, 89–100. [[CrossRef](#)]
47. Cunge, J.A. *Advances in Hydroinformatics*; Springer: Berlin, Germany, 2014; pp. 5–18. [[CrossRef](#)]
48. De Sousa, M.M.; de Oliveira, A.K.B.; Rezende, O.M.; de Magalhães, P.M.C.; Jacob, A.C.P.; de Magalhães, P.C.; Miguez, M.G. Highlighting the role of the model user and physical interpretation in urban flooding simulation. *J. Hydroinform.* **2022**, *24*, 976–991. [[CrossRef](#)]
49. Kötter, T.; Vafeidis, A.; Moghadas, M.; Asadzadeh, A.; Fekete, A. A multi-criteria approach for assessing urban flood resilience in Tehran, Iran. *Int. J. Disaster Risk Reduct.* **2019**, *35*, 101069. [[CrossRef](#)]
50. Miguez, M.G.; Battemarco, B.P.; De Sousa, M.M.; Rezende, O.M.; Veról, A.P.; Gusmaroli, G. Urban Flood Simulation Using MODCEL—An Alternative Quasi-2D Conceptual Model. *Water* **2017**, *9*, 445. [[CrossRef](#)]
51. Miguez, M.G.; Mascarenhas, F.C.B.; Veról, A.P. MODCEL: A Mathematical Model for Urban Flood Simulation and Integrated Flood Control Design. In Proceedings of the Convegno Nazionale Di Idraulica Urbana, Venezia, Italy, 21–24 June 2011; pp. 1–17.
52. Ouma, Y.O.; Tateishi, R. Urban Flood Vulnerability and Risk Mapping Using Integrated Multi-Parametric AHP and GIS: Methodological Overview and Case Study Assessment. *Water* **2014**, *6*, 1515–1545. [[CrossRef](#)]
53. Boulomytis, V.T.G.; Zuffo, A.C.; Alam Imteaz, M. Assessment of flood susceptibility in coastal peri-urban areas: An alternative MCDA approach for ungauged catchments approach for ungauged catchments. *Urban Water J.* **2022**, 1–13. [[CrossRef](#)]
54. De Morisson Valeriano, M.; de Fátima Rossetti, D. Topodata: Brazilian full coverage refinement of SRTM data. *Appl. Geogr.* **2011**, *32*, 300–309. [[CrossRef](#)]
55. Farr, T.G.; Kobrick, M. Shuttle radar topography mission produces a wealth of data. *Eos Trans. Am. Geophys. Union* **2000**, *81*, 583–585. [[CrossRef](#)]
56. IBGE. Censo 2010. Brazilian Institute of Geography and Statistics. 2010. Available online: <https://censo2010.ibge.gov.br/> (accessed on 10 April 2023).
57. IBGE. Grade Estatística. Brazilian Institute of Geography and Statistics: Statistic Grid. 2016. Available online: [https://geoftp.ibge.gov.br/recortes\\_para\\_fins\\_estatisticos/grade\\_estatistica/censo\\_2010/grade\\_estatistica.pdf](https://geoftp.ibge.gov.br/recortes_para_fins_estatisticos/grade_estatistica/censo_2010/grade_estatistica.pdf) (accessed on 22 June 2023).
58. Burrough, P.A.; McDonell, R.A. *Principles of Geographical Information Systems*; Oxford University Press: Oxford, UK, 1998; p. 190.

59. Nobre, A.D.; Cuartas, L.A.; Hodnett, M.; Rennó, C.D.; Rodrigues, G.; Silveira, A.; Waterloo, M.; Saleska, S. Height Above the Nearest Drainage—A hydrologically relevant new terrain model. *J. Hydrol.* **2011**, *404*, 13–29. [[CrossRef](#)]
60. Wilken, P.S. *Surface Drainage Engineering*, 1st ed.; CETESB: São Paulo, Brazil, 1978.
61. Horton, B.P.; Khan, N.S.; Cahill, N.; Lee, J.S.H.; Shaw, T.A.; Garner, A.J.; Kemp, A.C.; Engelhart, S.E.; Rahmstorf, S. Estimating global mean sea-level rise and its uncertainties by 2100 and 2300 from an expert survey. *NPJ Clim. Atmos. Sci.* **2020**, *3*, 18. [[CrossRef](#)]
62. World Bank. Climate Change Knowledge Portal [WWW Document]. Proj. Sea Lev. Rise. 2022. Available online: <https://climateknowledgeportal.worldbank.org/country/brazil/impacts-sea-level-rise> (accessed on 8 May 2023).
63. Tebaldi, C.; Ranasinghe, R.; Vousdoukas, M.; Rasmussen, D.J.; Vega-Westhoff, B.; Kirezci, E.; Kopp, R.E.; Sriver, R.; Mentaschi, L. Extreme sea levels at different global warming levels. *Nat. Clim. Chang.* **2021**, *11*, 746–751. [[CrossRef](#)]
64. Luiz-Silva, W.; Oscar-Júnior, A.C. Climate extremes related with rainfall in the State of Rio de Janeiro, Brazil: A review of climatological characteristics and recorded trends. *Nat. Hazards* **2022**, *114*, 713–732. [[CrossRef](#)]
65. Dereczynski, C.; Silva, W.L.; Marengo, J. Detection and Projections of Climate Change in Rio de Janeiro, Brazil. *Am. J. Clim. Chang.* **2013**, *2*, 25–33. [[CrossRef](#)]
66. Mascarenhas, F.C.B.; Miguez, M.G. Urban Flood Control through a Mathematical Cell Model. *Water Int.* **2002**, *27*, 208–218. [[CrossRef](#)]
67. Miguez, M.G.; de Magalhães, L.P.C.; Dearáújo, F.F. Stepping towards sustainable urban drainage practices at Acari River basin in Rio de Janeiro. *WIT Trans. Ecol. Environ.* **2009**, *122*, 305–316. [[CrossRef](#)]
68. Miguez, M.G.; de Magalhães, L.P.C. Urban Flood Control, Simulation and—An Integrated Approach. *Intech Open* **2010**, *2*, 64. [[CrossRef](#)]
69. Miguez, M.G.; Veról, A.P.; Battemarco, B.P.; Yamamoto, L.M.T.; de Brito, F.A.; Fernandez, F.F.; Merlo, M.L.; Rego, A.Q. A framework to support the urbanization process on lowland coastal areas: Exploring the case of Vargem Grande—Rio de Janeiro, Brazil. *J. Clean. Prod.* **2019**, *231*, 1281–1293. [[CrossRef](#)]
70. Rezende, O.M.; de Franco, A.B.R.; Oliveira, A.K.B.; Jacob, A.C.P.; Miguez, M.G. A Framework to Assess Urban Floods Resilience. In *New Trends in Urban Drainage Modelling: UDM 2018*; Mannina, G., Ed.; Springer: Cham, Switzerland, 2018; pp. 533–538. [[CrossRef](#)]

**Disclaimer/Publisher’s Note:** The statements, opinions and data contained in all publications are solely those of the individual author(s) and contributor(s) and not of MDPI and/or the editor(s). MDPI and/or the editor(s) disclaim responsibility for any injury to people or property resulting from any ideas, methods, instructions or products referred to in the content.